This article was downloaded by:
On: *25 January 2011*
Access details: *Access Details: Free Access*
Publisher *Taylor & Francis*
Informa Ltd Registered in England and Wales Registered Number: 1072954 Registered office: Mortimer House, 37-41 Mortimer Street, London W1T 3JH, UK

Liquid Crystals

Publication details, including instructions for authors and subscription information:
http://www.informaworld.com/smpp/title~content=t713926090

The effect of electric fields on light scattering in the isotropic phase of CE6/CE6R mixtures

Upindranath Singh[a]; Carlos Hunte[a]
[a] Department of Physics, University of the West Indies, Bridgetown, Barbados

To cite this Article Singh, Upindranath and Hunte, Carlos(2006) 'The effect of electric fields on light scattering in the isotropic phase of CE6/CE6R mixtures', Liquid Crystals, 33: 7, 841 — 847

To link to this Article: DOI: 10.1080/02678290600722890

URL: http://dx.doi.org/10.1080/02678290600722890

PLEASE SCROLL DOWN FOR ARTICLE

Full terms and conditions of use: http://www.informaworld.com/terms-and-conditions-of-access.pdf

This article may be used for research, teaching and private study purposes. Any substantial or systematic reproduction, re-distribution, re-selling, loan or sub-licensing, systematic supply or distribution in any form to anyone is expressly forbidden.

The publisher does not give any warranty express or implied or make any representation that the contents will be complete or accurate or up to date. The accuracy of any instructions, formulae and drug doses should be independently verified with primary sources. The publisher shall not be liable for any loss, actions, claims, proceedings, demand or costs or damages whatsoever or howsoever caused arising directly or indirectly in connection with or arising out of the use of this material.

Liquid Crystals, Vol. 33, No. 7, July 2006, 841–847

The effect of electric fields on light scattering in the isotropic phase of CE6/CE6R mixtures

UPINDRANATH SINGH* and CARLOS HUNTE
Department of Physics, University of the West Indies, P.O. Box 64, Bridgetown, Barbados

(*Received 15 July 2005; in final form 14 February 2006; accepted February 2006*)

The pretransitional back-scattering of circularly polarized light in CE6/CE6R blends was studied and the amplitude of the fluctuations in two of the five structural modes present in the isotropic phase of chiral nematic liquid crystals measured. From these measurements, the second order transition temperatures for these two modes were calculated. We found that both the chirality and the applied fields affect the fluctuations but the chiral effects seem to dominate over the field effects.

1. Introduction

Significant progress towards the understanding of phase transitions in highly chiral nematic liquid crystals stemmed from the realization that the order in such systems can be represented by a linear combination of five basic structural modes [1–3], all of which can fluctuate about their equilibrium value and hence scatter light. These modes, labelled $m=\pm 2$, ± 1 and 0, represent the planar spiral, conical spiral and achiral modes respectively [4, 5]. The Landau–de Gennes free energy for each of these modes vanishes at some temperature T_m^*. All T_m^* are lower than the transition temperature, T_c, and $T_2^* > T_1^*$.

The most direct way to measure fluctuations in the isotropic phase is to perform light scattering experiments. By using the Mueller matrix formalism, Hornreich and Shtrikman [2] have derived a general scattering matrix in terms of the amplitudes of the five modes and the scattering angle. In this approach, the input and output beams are expressed as 4×1 Stokes vectors. The connection between the two vectors can be expressed as a linear transformation whose sixteen coefficients form the 4×4 Mueller matrix from which all scattering properties of the sample can be determined.

In general, light is scattered from a combination of the five modes of the order parameter. However, a single mode can be probed by employing the back scattering of right (or left) circularly polarized light [R(L)CPL]; all other scattering geometries are sensitive to the fluctuations of more than one mode. If both incident and back-scattered beams are RCPL (LCPL) the $m=-2$ (m=+2) mode is excited and there is no contribution from the $m=\pm 1$ modes [2]. If the incident beam is RCPL (LCPL) and the back-scattered beams are LCPL (RCPL), coupling with the $m=0$ modes occurs. From such experiments, one can deduce the 2nd order transition temperatures, T_m^* as well as the pitch parameter (κ) [6] which plays a central role in the theory of Hornreich and Shtrikman. In addition, this paper represents the first report on the effect of electric fields on the back-scattering of circularly polarized light.

2. Theory

For a cholesteric liquid crystal, the Landau–de Gennes free energy to second order can be written as [2, 7, 8]:

$$F_2 = F_0 + \frac{1}{2}\int \mathrm{d}\mathbf{r}\Big[aQ_{\alpha\beta}^2 + b\left(\partial_\gamma Q_{\alpha\beta}\right)^2 + c\partial_\alpha Q_{\alpha\gamma}\partial_\beta Q_{\beta\gamma} - 2de_{\alpha\beta\gamma}Q_{\alpha\delta}\partial_\gamma Q_{\beta\delta}\Big] \qquad (1)$$

where $Q_{\alpha\beta}$ is the dielectric tensor representing the local order, $e_{\alpha\beta\gamma}$ is the Levi–Civita tensor, $a=a_0\,(T-T^*)$, the coefficients b, c and d are temperature-independent and T^* is the second order phase transition temperature of the racemic mixture. If the order parameter is expressed in terms of the five structural modes, equation (1) reduces to:

$$F_2 = F_0 + \frac{1}{2}\sum_m \int \mathrm{d}^3\mathbf{q}\left[a - mdq + \left[b + \frac{c}{6}\left(4 - m^2\right)\right]q^2\right] |\sigma^m(\mathbf{q})|^2 \qquad (2)$$

where m labels the mode, $\mathbf{q}$ is the wave vector of light and σ^m ($\mathbf{q}$) is the amplitude of the mode. There is a

---

*Corresponding author. Email: usingh@uwichill.edu.bb

Liquid Crystals
ISSN 0267-8292 print/ISSN 1366-5855 online © 2006 Taylor & Francis
http://www.tandf.co.uk/journals
DOI: 10.1080/02678290600722890

specific value of q, which minimizes the free energy of each mode.

By using the equipartition theorem, the mean-square fluctuation of the modes can be written as:

$$\langle \sigma^m(\mathbf{q})\sigma^m(-\mathbf{q})\rangle = \delta_{\mathbf{q},\,-\mathbf{q}}\frac{(k_\mathrm{B}T)/2}{\tau^m(\mathbf{q})} \tag{3}$$

where:

$$\begin{aligned} \tau^{\pm 2}(q) &= a + bq^2 \mp 2dq \\ \tau^{\pm 1}(q) &= a + (b+c)q^2 \mp 2dq \\ \tau^{0}(q) &= a + \left(b + \frac{2}{3}c\right)q^2. \end{aligned} \tag{4}$$

Following the procedure of Hornreich and Shtrikman [2], one can deduce expressions for the scattered intensity in any one of the four possible scattering configurations. For RCPL incident and RCPL detected, the intensity is given by:

$$I(\mathbf{q}) = \frac{k_\mathrm{B}T}{2}\left[\frac{2c^4}{3\tau^0} + \frac{(1-s)^4}{\tau^2} + \frac{(1+s)^4}{\tau^{-2}}\right] \tag{5}$$

where $s=\sin(\theta/2)$ and $c=\cos(\theta/2)$ (θ is the scattering angle). For LCPL incident and LPCL detected, a similar calculation yields:

$$I(\mathbf{q}) = \frac{k_\mathrm{B}T}{2}\left[\frac{2c^4}{3\tau^0} + \frac{(1+s)^4}{\tau^2} + \frac{(1-s)^4}{\tau^{-2}}\right]. \tag{6}$$

If the incident and scattered beams have opposite states of polarization, the intensity is given by the expression:

$$I(\mathbf{q}) = \frac{k_\mathrm{B}T}{2}\left[\frac{2(c^2+2)^2}{3\tau^0} + \frac{4c^2}{\tau^1} + \frac{4c^2}{\tau^{-1}} + \frac{(s^2-1)^2}{\tau^2} + \frac{(s^2-1)^2}{\tau^{-2}}\right]. \tag{7}$$

For the scattering angle used in this experiment, $\theta=175°$, the coefficients of the first and second terms in equation (5) are 1.5×10^{-7} and 5×10^{-14} times that of the third term, respectively. Thus, for a right handed system, the contribution of the $m=-2$ mode to the backscattering is much greater than that of either the $m=2$ or $m=0$ mode. The situation is reversed for a left-handed system.

The temperature–chirality phase diagrams for CE6/CE6R mixtures deduced from optical and thermal techniques have been previously published [9, 10]. These two techniques have yielded phase diagrams that are topologically consistent. The main feature includes an increase in the number of blue phases with increasing chirality. It has been established that the temperature widths of both BPI and BPIII become wider with increasing chirality, while BPII becomes narrower and vanishes with high chirality. This disappearance of BPII is observed in chiral blends of CE2-CE2R. CE2 is a chiral material with a pitch much shorter than CE6 [9]. We have also deduced this phase diagram (see figure 1) from optical activity data and the results are consistent with those previously published [11].

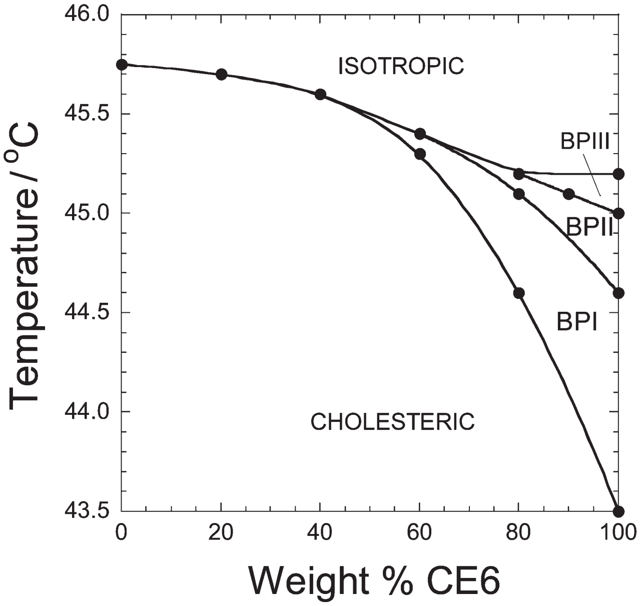

Figure 1. Temperature–chirality phase diagram for CE6/CE6R mixtures.

3. Experiment

The optical system (figure 2) was designed to measure fluctuations from just one mode. Circularly polarized light was generated by passing horizontally polarized light (from a He-Ne laser, 633 nm) through a quarter-wave plate ($\lambda/4$) whose fast axis was oriented at 45° to the x-axis (−45° yields LCPL and +45° yields RCPL). The incident light was focused onto the sample using a long focal length convex lens. The back-scattered beam is a mixture of RCPL and LCPL since it contains contributions from the sample as well as reflections from non-chiral materials (for example, RCPL is reflected as LCPL from glass). This mixture of RCPL and LCPL was decomposed into two orthogonal plane polarized beams with the help of a second quarter-wave plate whose orientation was the same as the first. LCPL (RCPL) was then detected by passing the light through a horizontal (vertical) polarizer.

The sample was housed in a cylindrical glass cell (2.5 cm path length), placed in a high temperature oven.

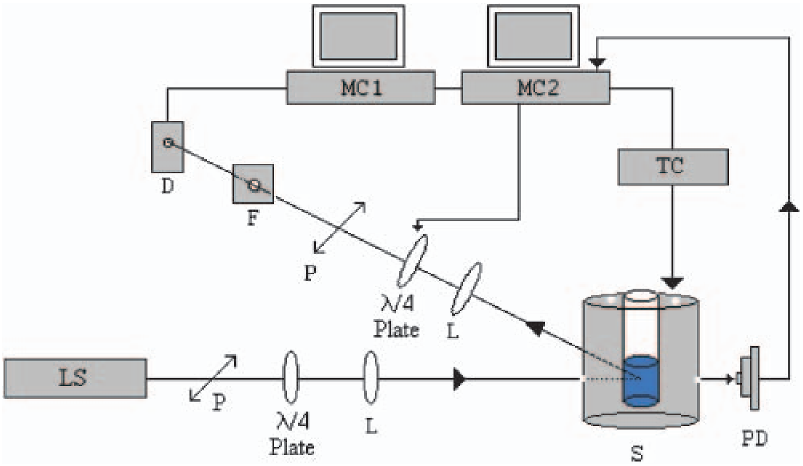

Figure 2. The scattering geometry used to detect fluctuations from a single mode. The symbols are: LS (light source); P (polaroid); $\lambda/4$ plate (quarter-wave plate); L (lens); F (filter); D (detector); MC (microcomputer); TC (temperature controller); S (sample); PD (photodiode).

Temperature control to ± 0.01 K or better was achieved with an Instec MK1 temperature controller. The background intensity was measured after heating the sample to the isotropic phase and allowing to equilibrate for about three hours. This background intensity was subtracted from each intensity measurement. The scattered intensity and temperature were recorded at 0.05 K intervals as the sample was cooled at a rate of $0.6\,\mathrm{K\,h^{-1}}$.

The experiment was repeated with constant d.c. fields applied across the sample. Custom designed electrodes (1 cm spacing) were inserted into glass cells and voltages up to 4 kV were applied. We are aware of the build up of charges for d.c. fields, but high a.c. fields were not available.

The samples used in this study were mixtures of the chiral compound CE6 and its racemate CE6R which were obtained from Merck Ltd, UK. By mixing CE6 and CE6R one ensures that only the chirality of the samples is changed throughout the experiments. The structure of CE6 is shown in figure 3 and the scattering geometry in figure 4.

4. Results and discussion

According to equation (3), a graph of back-scattered intensity versus temperature should vary as $[T - T^*_{\pm 2}]^{-1}$ in the isotropic phase. Thus, a plot of inverse intensity for both $m=-2$ and $m=+2$ modes should yield two parallel lines with the same T_c but different T^* (given by the intercepts on the temperature axis). This is illustrated in figure 5, where the straight

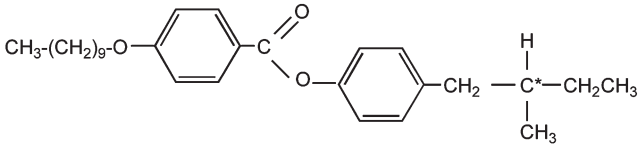

Figure 3. Chemical structure of CE6.

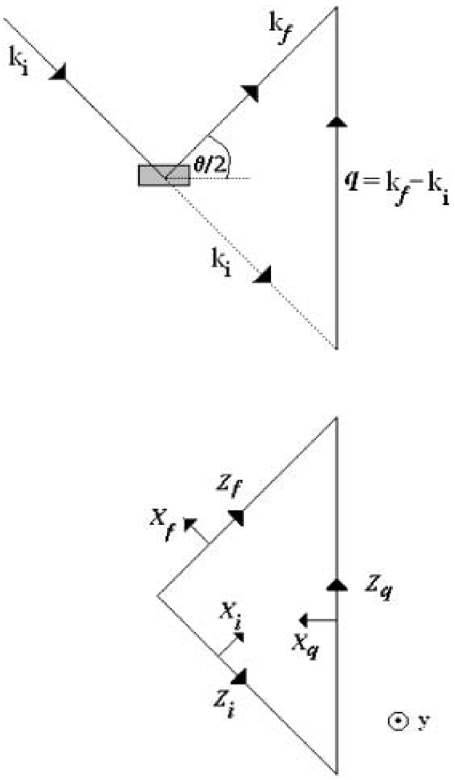

Figure 4. Top: schematic view of scattering plane, showing the wave vectors for the incident and scattered light and the scattering wave vector **q**. Bottom: the coordinate system associated with each of the wave vectors.

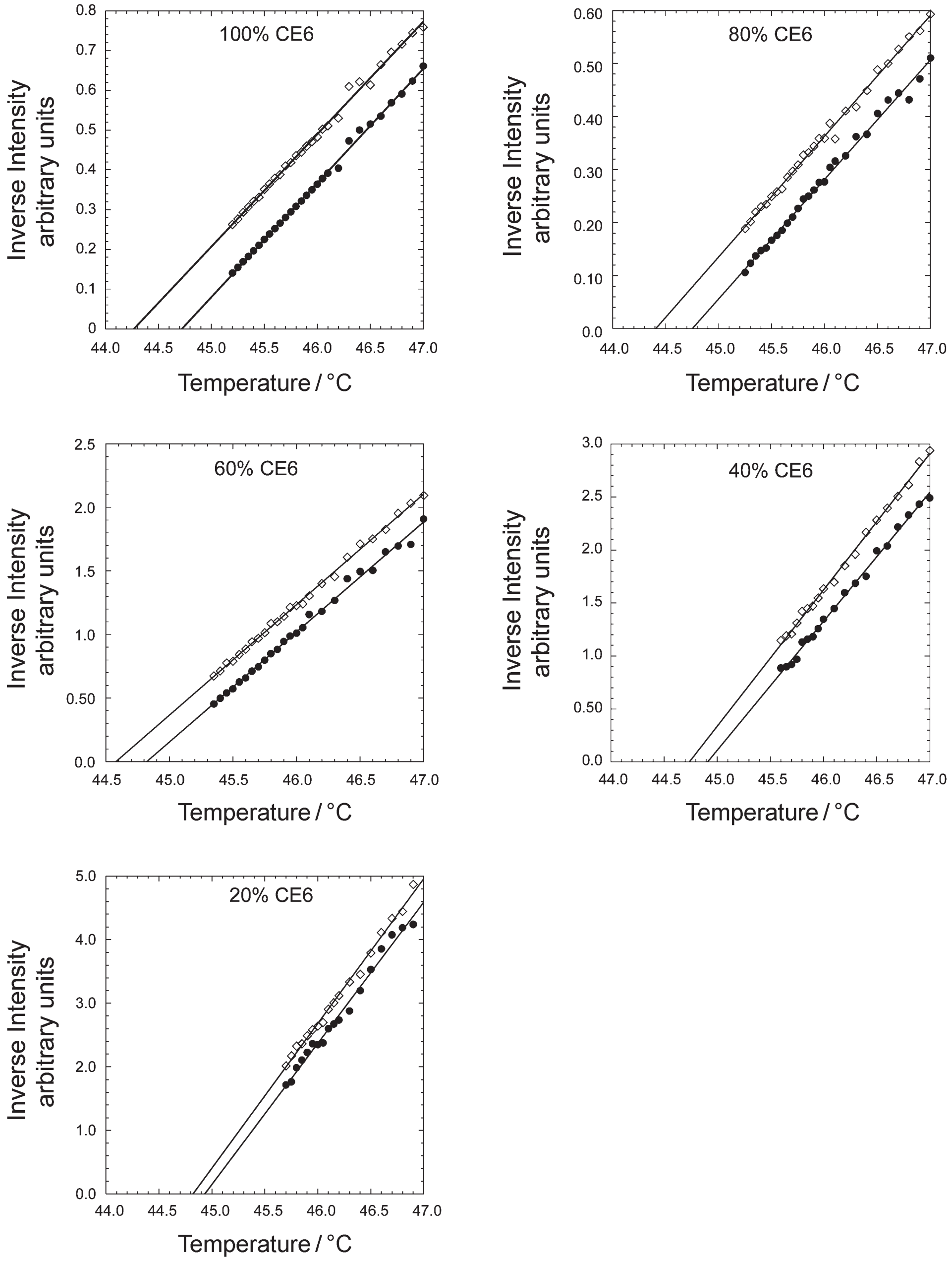

Figure 5. The reciprocal of the back-scattered intensity for CE6-CE6R mixtures. The solid circles correspond to the $m=-2$ modes and the open squares to the $m=+2$ modes. The solid lines are least squares fit to equation (8).

lines are least-squares fit to the expression:

$$I = I_0 + K\left[T - T^*_{\pm 2}(q)\right]^{-1} \qquad (8)$$

where I is the back-scattered intensity and K, I_0 and T^* are fitting parameters. The difference between the highest and lowest second order transition temperatures for a right-handed system (such as CE6) is given by:

$$T^*_{-2} - T^*_2 = \frac{-4bqq_0}{a_0} \text{ where } (q_0 = 2\pi/\text{Pitch}). \qquad (9)$$

Hence, the separation of the inverse intensity lines should increase with increasing chirality. This is indeed observed in the five plots of figure 5, and the data is thus consistent with theoretical predictions. Also, the slopes of the least-squares lines lie within ±5% of the mean over the entire range considered.

We estimated the ratio b/a_o using the experimentally determined values of the second order transition temperatures and the cholesteric pitch. However, the cholesteric pitch quoted in the manufacturers data sheet

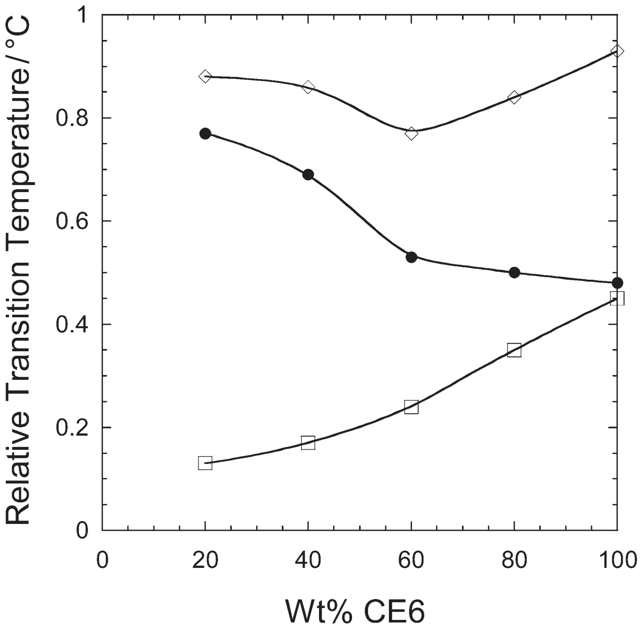

Figure 6. Relative transition temperature versus temperature for CE6-CE6R mixtures (□ represents $T^*_{-2}-T^*_{+2}$, • represents $T_c-T^*_{-2}$ and ◇ represents $T_c-T^*_{+2}$).

and that measured by Yang and Crooker [9] are 0.23 and 0.16 μm, respectively. By using both values, we found that b/a_o varies from 1.4×10^{-16} to $1.8\times10^{-16}\,\mathrm{m^2\,K}$. These values are consistent with that obtained by Battle *et al.* [12], who used optical activity data in their calculations.

We could not determine the value of T^*_{-2} or T^*_{+2} for CE6R owing to very weak reflections from this sample. Such weak reflections in materials of low chirality have been observed previously [13]. The difference $T^*_{-2}-T^*_{+2}$ should be proportional to the chirality (q_o) provided the other parameters remain constant. To a fairly good approximation, the chirality is proportional to the weight % of CE6. This increase in $T^*_{-2}-T^*_{+2}$ with increasing chirality is clearly evident (see figure 6). The differences between T_c and the second order transition temperatures are also shown in figure 6. The non-linear dependence in the data has been attributed to variation in the parameters a_0 and b as different amounts of CE6 and CE6R are mixed together [13].

The schematic representation of structural modes of the order parameter tensor, which is represented by an ellipsoid of revolution, is shown in figure 7 [5]. The arrows represent the magnitude and direction of the largest principal axis. For $m=0$, the ellipsoid alternates between horizontal and vertical. For $m=1$, the largest principal axis of the tensor rotates about, and lies at 45° to, the horizontal axis. The mode $m=2$ is the largest principal axis of the order parameter tensor and rotates about, and is perpendicular to, the horizontal axis. The arrows represent the projection of the principal axis on the plane of the diagram with the solid parts of the arrows above the plane of the diagram and the dashed part below.

In our scattering configuration (figure 4), the light propagates along the z-direction and the applied field is in the x-direction. Thus, from figure 7, the electric field is expected to affect the fluctuations of all modes, but our experiment is designed to measure the fluctuations of just the $m=\pm2$ modes. However, if mode coupling is invoked by the application of fields then the scattering of $m=\pm2$ modes could be affected. The choice of CE6 and CE6R was based simply on availability. However, this might not be the ideal combination owing to the weak dielectric anisotropy of these materials. In addition, it is somewhat impractical with this back scattering configuration to have electrodes closer than 1 cm apart; this limits the magnitude of the fields which can be applied.

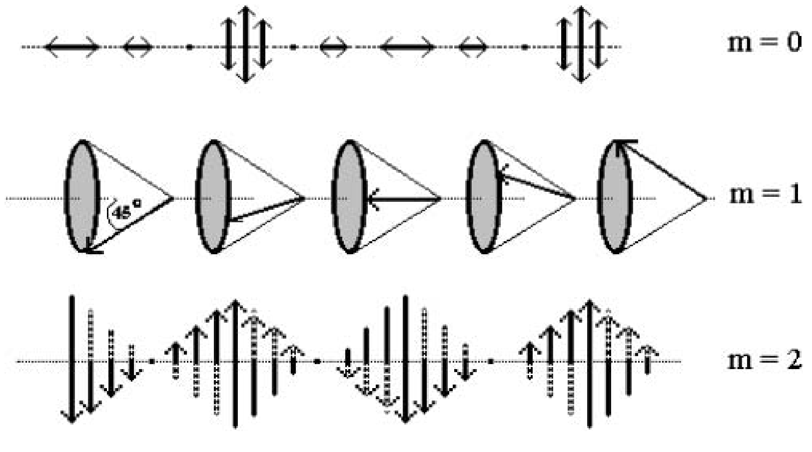

Figure 7. Schematic representations of the normal modes of a chiral nematic liquid crystal.

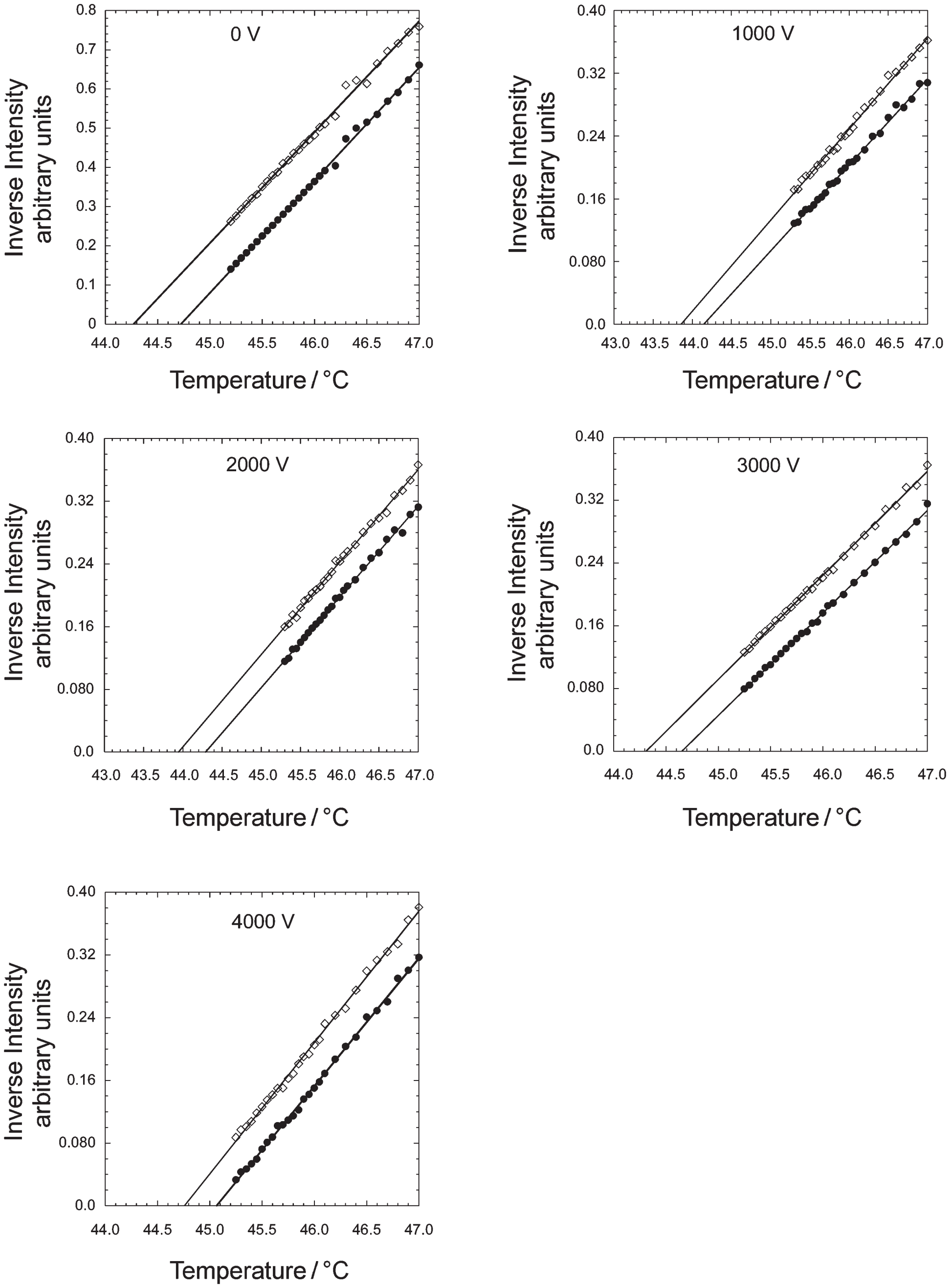

Figure 8. The reciprocal of the back scattered intensity for CE6 at various applied fields applied perpendicular to the propagation of light. The solid circles correspond to the $m=-2$ modes, the open squares to the m=+2 modes.

The effect of electric fields on the differences in the second order transition temperatures in pure CE6 is shown in figure 8. There is an initial decrease in $T^*_{-2}-T^*_{+2}$ (from 0.45 to 0.3 ± 0.05 K) when $1\,\text{kV}\,\text{cm}^{-1}$ is applied. This decrease may be attributed to the reduction in pretransitional chiral order. Kang and Dunmur [5] investigated the effect of a.c. electric fields on the pretransitional optical activity of CE6 and found little variation when either parallel or transverse fields of $1\,\text{kV}\,\text{mm}^{-1}$ were applied. This was attributed to the small (positive) dielectric anisotropy of CE6. However, optical activity experiments in CE6 probe the response of only the $m=\pm1$ modes. By comparison, Hunte *et al.* [14] found that d.c. fields of $\sim270\,\text{V}\,\text{mm}^{-1}$ were sufficient to destroy contributions from the $m=\pm2$ modes in the highly chiral CB15, while fields three times greater had no discernable effect on the $m=\pm1$ modes (because CB15 is highly chiral, both modes contribute

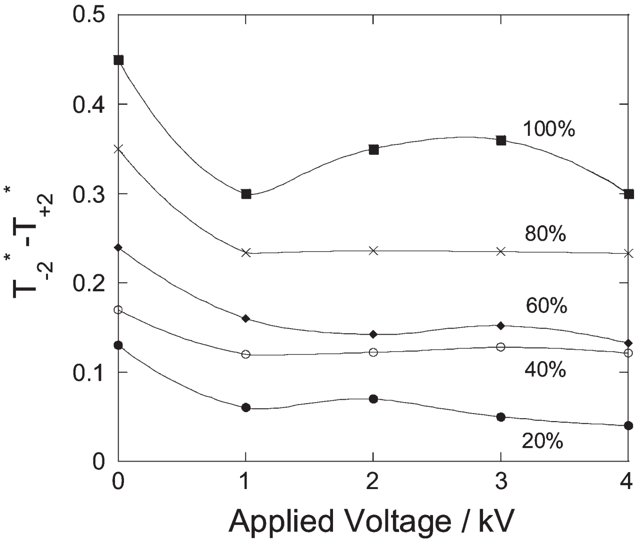

Figure 9. The voltage dependence of the second order transition temperatures at various chiralities. The percentages represent the weight fraction of CE6.

to the optical activity). Also, CB15 possesses a large and positive dielectric anisotropy and thus couples strongly to applied fields. We applied a field one tenth that of Kang and Dunmur [5] but observed a 33% decrease in $T^*_{-2} - T^*_{+2}$. Thus, one can intuitively infer that the $m = \pm 2$ modes couple to applied fields to a greater extent than the $m = \pm 1$ modes.

The difference $T^*_{-2} - T^*_{+2}$ is essentially unchanged if voltages greater than 1 kV are applied. When a field is applied, the scattered intensity of each mode increases but the difference in the second order transition temperatures remains unaffected. It was expected that as the voltages increased above 1 kV cm^{-1}, the chiral fluctuations would be progressively reduced and the separation of the parallel lines in figure 8 should decrease. Since this was not observed, this might mean than the thermal effects which oppose field effects still persist even when 4 kV was applied.

The combined effects of chirality and applied fields on the difference in the second order transition temperatures are captured in figure 9. For each mixture, the same trend is observed, namely a considerable decrease in $T^*_{-2} - T^*_{+2}$ initially which is not enhanced by further increase in the strength of the applied field. We have studied the effects of applied d.c. fields on the pretransitional optical activity in CB15 [14] and found a large field-induced effect. Unlike CE6, CB15 has a large dielectric anisotropy, explaining the difference in the two results. Kang and Dunmur [5] found little change in the pretransitional optical activity of CE6, even though they used a.c. fields in their study. Hence, we believe that the weak field-effects we observed are due to the small dielectric anisotropy of CE6.

5. Conclusion

We have shown that it is possible to scatter light from the fluctuations of a single mode even in low chirality nematic liquid crystal systems and hence determine the second order transition temperatures. Both the chirality and the applied fields affect the fluctuations responsible for light scattering, but the chiral effects seem to dominate over the field effects.

The zero-field results are consistent with theoretical predictions, in that a plot of inverse intensity versus temperature yields two parallel lines with the same T_c but different T^*. Also, the separation of these lines increases with increasing chirality, as expected. If optical activity and light scattering data are compared, one can deduce that the $m = \pm 2$ modes couple to a greater extent that the $m = \pm 1$ modes.

The pretransitional chiral order was reduced but never completely eliminated by the application of 4 kV in even the most chiral sample (CE6). There is no evidence of the applied field inducing mode coupling between the $m = 0$ and $m = \pm 2$ modes since there is no deviation from linearity in the data even near T_c, where fluctuations for each mode are expected to be the greatest.

References

[1] S.A. Brazovski, S.G. Dmitriev. *Zh. eksp. teor. Fiz.*, **69**, 979 (1975); *Sov. Phys. JETP*, **42**, 497 (1975).

[2] R.M. Hornreich, S. Shtrikman. *Phys. Rev. A*, **28**, 1791 (1983).

[3] S.A. Brazovski, V.M. Filev. *Zh. eksp. teor. Fiz.*, **75**, 1140 (1978); *Sov. Phys. JETP*, **48**, 573 (1978).

[4] P.J. Collings. *Mod. Phys. Lett.*, **B6**, 425 (1992).

[5] J.S. Kang, D.A. Dunmur. *Phys. Rev. E*, **51**, 2129 (1995).

[6] U. Singh, L.L. Moseley. *J. Phys. II Fr.*, **5**, 919 (1995).

[7] H. Grebel, R.M. Hornreich, S. Shtrikman. *Phys. Rev. A*, **30**, 3264 (1984).

[8] H. Grebel, R.M. Hornreich, S. Shtrikman. *Phys. Rev. A*, **28**, 1114 (1983).

[9] D.K. Yang, P.P. Crooker. *Phys. Rev. A*, **35**, 4419 (1987).

[10] G. Voets, W. van Dael. *Liq. Cryst.*, **14**, 617 (1993).

[11] C. Hunte. PhD thesis, University of the West Indies (2003).

[12] P.R. Battle, J.D. Miller, P.J. Collings. *Phys. Rev. A*, **36**, 369 (1987).

[13] J.E. Wyse, P.J. Collings. *Phys. Rev. A*, **45**, 2449 (1992).

[14] C. Hunte, U. Singh, P. Gibbs. *J. Phys. II Fr.*, **6**, 1291 (1996).